water

MDPI

Supplementary Material

Photocatalytic Bactericidal Performance of $LaFeO_3$ under Solar Light in the presence of Natural Organic Matter: Spectroscopic and Mechanistic Evaluation

Birben Nazmiye Cemre [1], Lale Ezgi [1], Pelosato Renato [2], Turkten Nazli [3], Natali Sora Isabella [2] and Bekbolet Miray [1]

[1] Institute of Environmental Sciences, Bogazici University, Istanbul, Turkey.
[2] Department of Engineering and Applied Sciences, University of Bergamo, Dalmine, Italy
[3] Department of Chemistry, Faculty of Arts and Sciences, Kirsehir Ahi Evran University, Kirsehir, Turkey.

Kinetic Modeling

Logarithmic decay profiles of *E. coli* cell counts indicated that inactivation kinetics could be well-expressed by the first-order model:

$$\text{Rate (R)} = -dN/dt = kN$$

R: first-order rate (CFU/mL min),
N: *E. coli* count, CFU/mL at time t,
t: irradiation time, min,
k: first-order reaction rate constant, min^{-1}.
Half-life ($t_{1/2}$, min) could easily be calculated by the following equation, $t_{1/2} = 0.692/k$.

1. Spectroscopic Characterization of NOM Compounds

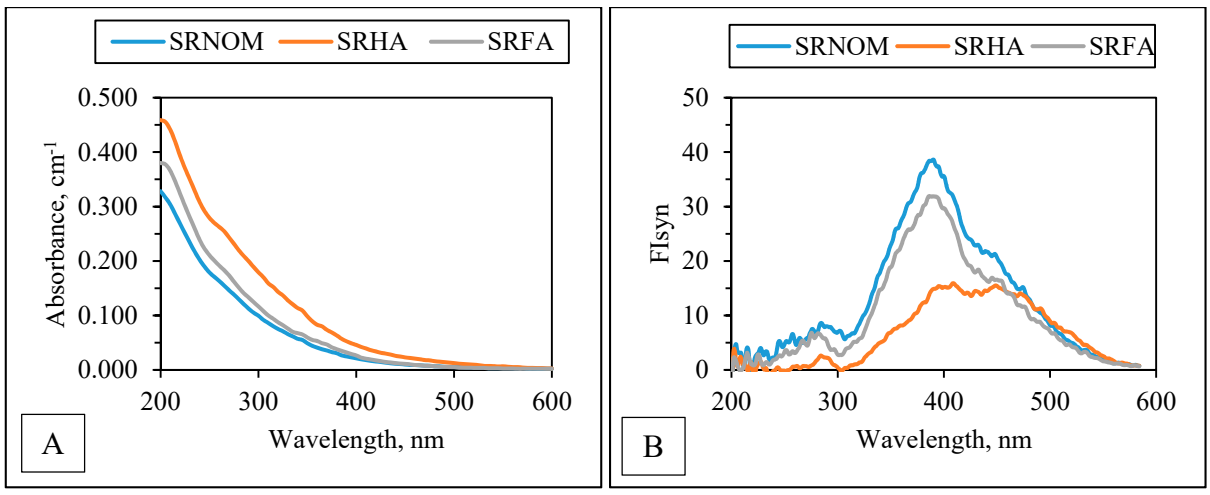

Figure S1. UV-vis (**A**) and synchronous scan fluorescence (**B**) spectral features of NOM compounds.

Table 1. Specified and specific UV-vis and fluorescence parameters of NOM compounds.

NOM origin	$Color_{436}$	UV_{365}	UV_{280}	UV_{254}	FI_{syn}	DOC	$SUVA_{254}$	SFI_{syn}
SRNOM	0.014	0.041	0.132	0.175	14.8	4.19	4.18	3.53
SRHA	0.035	0.092	0.237	0.287	13.7	3.95	7.27	3.47
SRFA	0.013	0.046	0.155	0.205	11.9	4.52	4.53	2.63

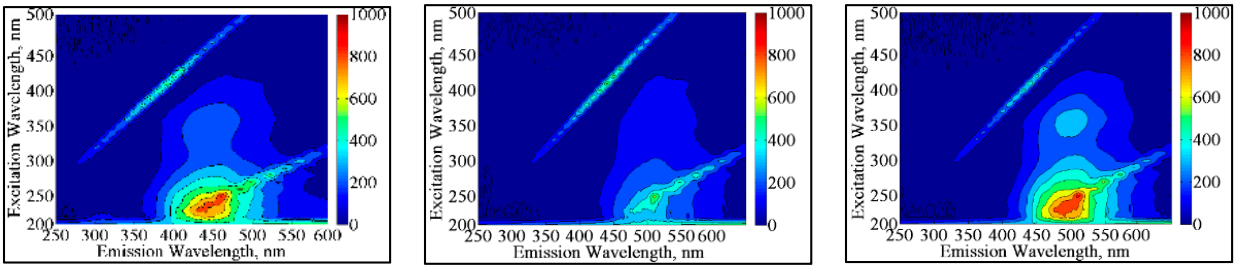

Figure S2. EEM fluorescence spectral features of IHSS NOM compounds: (**a**) SRNOM; (**b**) SRMA; (**c**) SRFA.

2. Acidic Functional Groups of NOM Compounds

Table S2. Acid functional groups of NOM compounds.

	Carboxyl	Phenolic	Q_1	$LogK_1$	n_1	Q_2	$LogK_2$	n_2
SRNOM	9.85	3.94	10.57	3.94	3.60	2.61	9.74	1.19
SRHA	9.13	3.72	9.74	4.35	3.30	4.48	10.44	1.73
SRFA	11.17	2.84	11.66	3.76	3.24	2.05	9.84	1.45

Carboxyl is the charge density (meq/g C) at pH 8.0; Phenolic is two times the change in charge density (meq/g C) between pH 8.0 and pH 10.0. The overall charge density (in meq/g C) of a humic substance increases systematically with pH (or with the concentration of H^+). The equation on the right, known historically as a modified Henderson-Hasselbalch equation for two classes of binding sites, was used to fit titration data and obtain the set of model fitting parameters in this table. The fitting parameters of the model were obtained by a nonlinear least-squares fit of the model to aggregated sets of replicate titration data. Q_1 and Q_2 are the maximum charge densities of the two classes of binding sites, Log K_1 and Log K_2 are the mean log K values for proton binding by the two classes of sites, and n_1 and n_2 are empirical parameters that control the width (in log K) of a class of proton binding sites. N is the number of fitted titration data points, and RMSE is the root mean-square error for fitting this model to the data (see Reference). This model, also known in more recent literature as a Langmuir-Freundlich equation, is the primary building block of the NICA class of models.

http://humic-substances.org/acidic-functional-groups-of-ihss-samples/ (accessed on 03 March 2021)

3. Photochemical and Photocatalytic Reactions Taking Place in the Presence of *E. coli* and NOM Analogue Compounds:

Based on this system description, "bacteria, organic matter and photocatalyst" consortium was subjected to irradiation *i.e.* photocatalysis. Simultaneously operating various degradation pathways could be described as; i. photolytic action on sole *E. coli* and photolysis of sole NOM analogue compounds, ii. photolytic action on "*E. coli* and NOM analogue compounds" binary system, iii. photocatalysis of sole *E. coli*, photocatalysis of sole NOM analogue compounds, and iv. photocatalysis of binary system composed of "*E. coli* and NOM analogue compounds".

NOM compounds mainly express a supramolecular structure composed of diverse structural groups expressing photosensitization properties that could form radical species such as $HO^{\bullet}$, $^1O_2$ and triplet states as ^{3}NOM*. ^{3}NOM* could further react through electron or hydrogen transfer oxidation mechanisms [1–3].

NOM + hν → ^{1}NOM* → ^{3}NOM* excitation followed by inter-system crossing

$^{3.}$ $NOM^* + O_2 \rightarrow NOM + {}^1O_2$

$^{3.}$ $NOM^* + H_2O \rightarrow NOM\text{-}H^* + HO^\bullet$

$^{3.}$ $NOM^* \rightarrow {}^3NOM^{\bullet+} + e^-$

$NOM^* + SC + h\nu \rightarrow NOM^{\bullet+} + SC(e^-)$

Electron trapping by semiconductor particles (SC) reduces e^-/h^+ recombination rate thereby indirectly enhances ROS formation. On the other hand, decrease of $HO^\bullet$ generation by NOM sub-fractions was reported for various photocatalysts (TiO_2, ZnO, and Fe_2O_3) with FA inhibiting $HO^\bullet$generation more than HA [55]. Singlet oxygen generation rate was dependent both on NOM and photocatalyst type. FA was more efficient than HA. Deactivation pathway of $^1O_2$ in the solution bulk proceeds through collisions with H_2O. $^1O_2$ has a micro-heterogeneous distribution within NOM matrix and could have higher concentrations when confined in the hydrophobic sites therefore possibly could only react in the vicinity of these centers. Hydrophobic cores would be more abundant in high molecular weight fractions of NOM.

Formation of reactive oxygen species:

Exposure of natural waters to solar irradiation produces ROS *i.e.* $HO^\bullet$, $^1O_2$, $O_2^{\bullet-}$, $HO_2^\bullet$ as well as e_{aq}^- via various reactions. Production of singlet oxygen $^1O_2$ [4] and hydrated electron e_{aq}^- [5] have been very well documented [6].

$O_2 + e_{aq}^- \rightarrow {}^1O_2$
$O_2 + e_{aq}^- \rightarrow O_2^{\bullet-}$
$O_2 + e_{aq}^- + H^+ \rightarrow HO_2^\bullet$
$HO_2^\bullet \rightarrow H^+ + O_2^{\bullet-}$ $\quad pK_a = 4.8$
$O_2^{\bullet-} + 2H^+ + e^- \rightarrow H_2O_2$
$H_2O_2 + e^- \rightarrow HO^\bullet + OH^-$
$HO^\bullet + e^- \rightarrow H_2O$

Reaction of $HO_2^\bullet$ and $O_2^{\bullet-}$ leading to the formation of H_2O_2 preferentially predominates over slow termination reactions in between two $HO_2^\bullet$ or two $O_2^{\bullet-}$ radicals

$$HO_2^\bullet + O_2^{\bullet-} + H^+ \rightarrow H_2O_2 + O_2$$

Upon solar light simulated irradiation conditions, the above given reactions (reaction numbers) and reactions (reaction numbers) occur leading to enhanced ROS formation complementary to those produced by photocatalysis. Therefore, under highly oxidizing conditions inactivation of *E. coli* as well as degradation of organic matter simultaneously take place.

4. FTIR Spectral Features

Table S3. Fourier Transform Infrared spectroscopic bands related to *E. coli* (italics) and NOM.

Band, cm^{-1}	**Assignment**
3450–3300	Associated O-H stretching (alcohols, phenols and carboxylic groups), N–H stretching (trace/minor), hydrogen-bonded OH
3400–3600 *~3500*	*Amide A, N–H stretching vibration mostly related to hydrogen bonding*
3100	*Amide B, N–H stretching vibration related amide II*
3080–3030	Aromatic C–H stretching
2950–2840	*Asymmetric and symmetric aliphatic C-H stretching vibrations (CH_3 and CH_2) mainly referred to lipids*
2935–2925, 2850	Asymmetric and symmetric C-H stretching of CH_2 group
1725–1710	C=O stretching of carboxylic groups (COOH, aldehydes and ketones)
1760–1600	*C=O and C–N stretching vibrations of amide I groups*
1660–1630	C=O stretching of amide groups (amide I band), C=O of quinone and/or H-bonded conjugated ketones
1620–1600 1640–1600	Aromatic C=C skeletal vibrations, symmetric stretching band of COO^-, C=O stretching in cyclic and alicyclic compounds, ketones and quinones
1620	*H–O stretching vibration related to H_2O absorption*
1540–1510 1512–1506	N–H deformation and C=N stretching (amide II band), aromatic C=C stretching
1575	Asymmetric stretching band of COO^- in carboxylic acid salts, *Aspartate or glutamate carboxylate stretching*
1470	*δ(CH_2) scissor*
1460–1440	Aliphatic C–H deformation
1420	C=N stretching of primary amides (amide III band)
1400–1380 1420–1415	Asymmetric stretching of COO^-, O–H deformation and C–O stretching of phenolic OH
1385 1380	Symmetrical stretching of COO^- in carboxylic acid, NO_3^-(aq) –H bending of CH_2 and CH_3 groups, asymmetric stretching of COO^-
1260–1200 1270–1260	C–O stretching and OH deformation of COOH, C–O stretching of aryl ethers and phenols
1280–1200	*Asymmetric and symmetric PO_2^- stretching vibrations of nucleic acid*
1290–1280	*Amide III*
1200–950	*Vibrations of the sugar rings of LPS*
1170	*C–O stretching vibration related to ring of carbohydrates*
1120–1140	*Asymmetric C–O–C stretching vibration of glycosidic linkage*
1085	*Symmetric PO_2^- band of DNA*
1060–1040	*Symmetric δ(COH) stretching vibration of carbohydrates*
975–775	*Out-of-plane bending of aromatic C–H*
966	*Asymmetric C–N stretching*
660–621	S-O stretching vibration of sulfonic groups

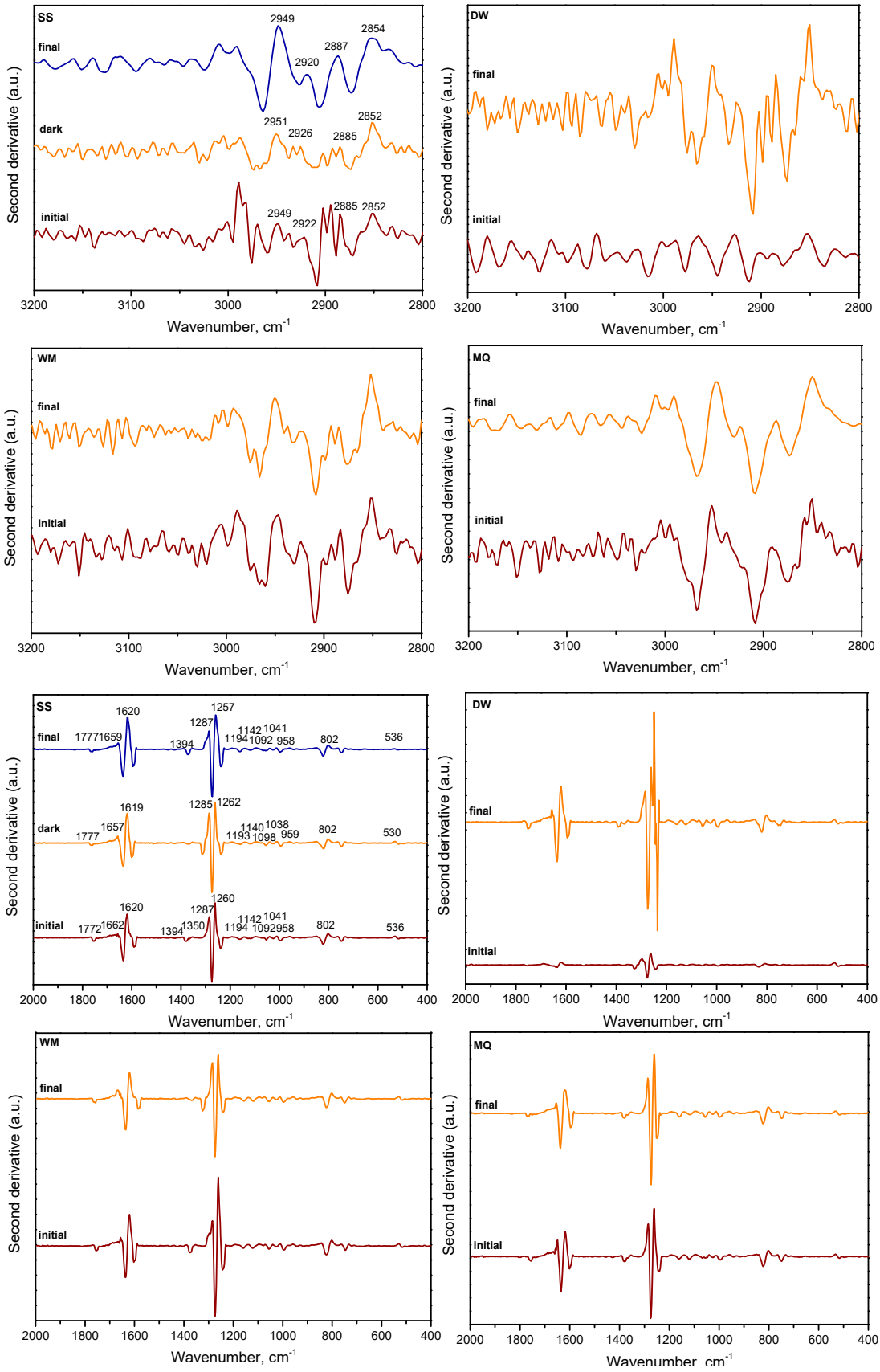

Figure S3. Second derivative FTIR spectra of *E. coli* and LF under various conditions in the absence of NOM compounds prior to (initial) and following (final) SPCI.

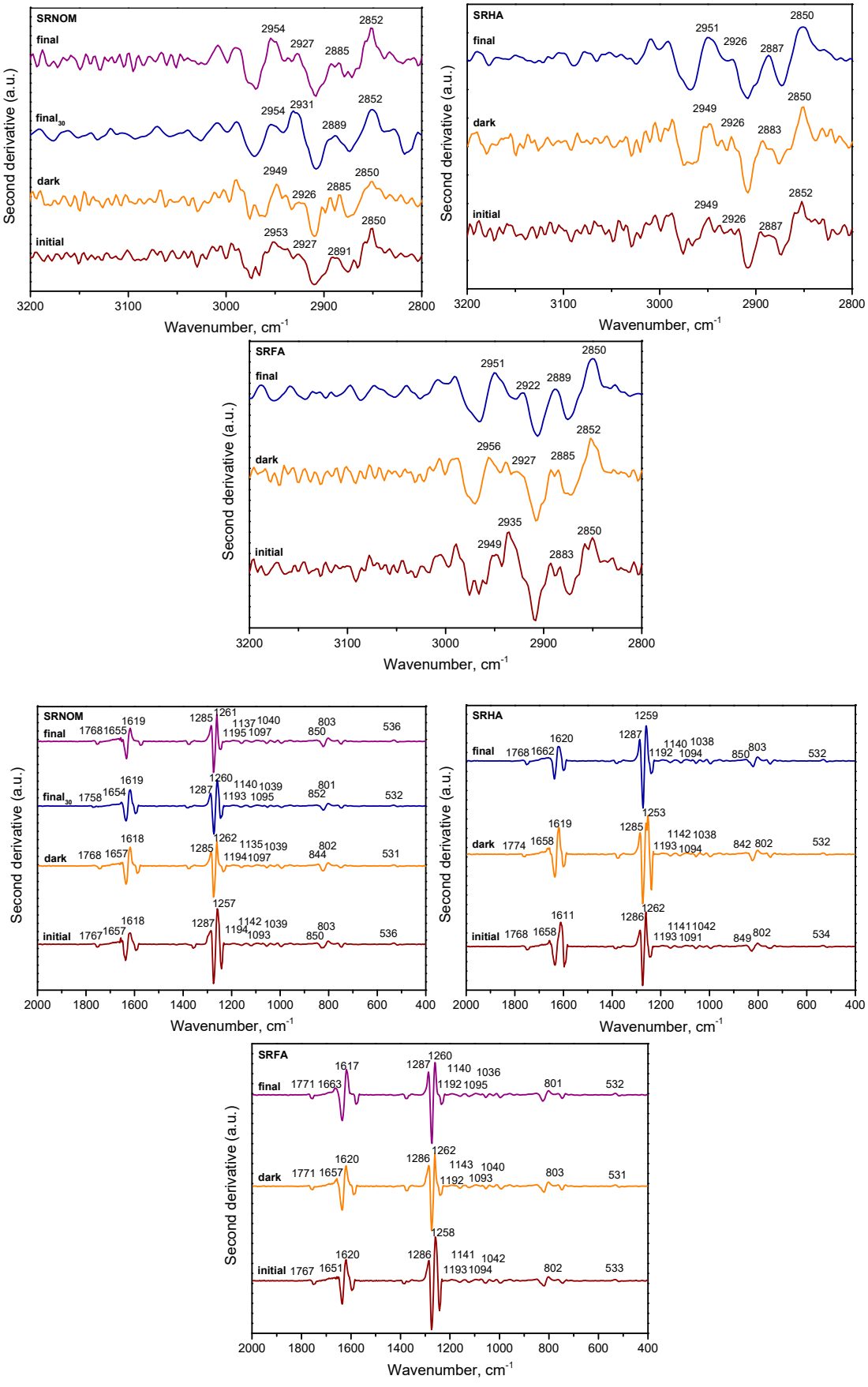

Figure S4. Second derivative FTIR spectra of *E. coli* and LF under various conditions in the presence of NOM compounds prior to (initial) and following (final) SPCI.

5. Correlation Between PARAFAC Component C1 and Protein Content Prior to and Following Solar Photocatalytic Inactivation of *E. coli* in the Absence/Presence of NOM

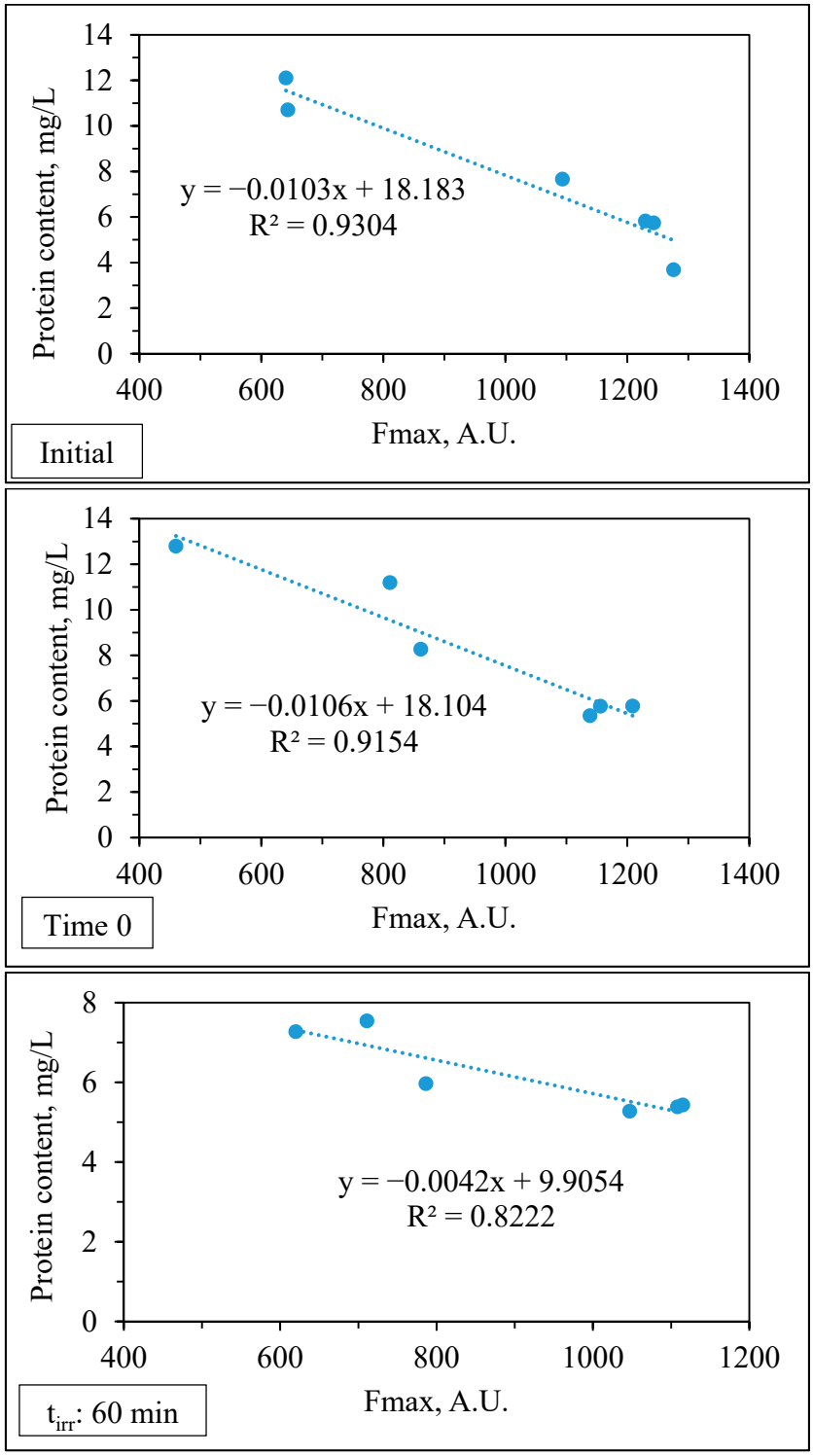

Figure S5. Correlation between Fmax values of PARAFAC component C1 and protein contents prior to and following solar photocatalytic inactivation of *E. coli* in the absence/presence of NOM.

References

1. Goldstone, J.V.; Pullin, M.J.; Bertilsson, A.; Voelker, B.M. Reactions of hydroxyl radical with humic substances: Bleaching, mineralization, and production of bioavailable carbon substrates. *Environ. Sci. Technol.* **2002**, *36*, 364–372.
2. Li, Y.; Niu, J.; Shang, E.; Crittenden, J.C. Influence of dissolved organic matter on photogenerated reactive oxygen species and metal-oxide nanoparticle toxicity. *Water Res.* **2016**, *98*, 9–18.
3. Vione, D.; Falletti, G.; Maurino, V.; Minero, C.; Pelizzetti, E.; Malandrino, M.; Ajassa, R.; Olarui, R.-I.; Arsene, C. Sources and sinks of hydroxyl radicals upon irradiation of natural water. *Environ. Sci. Technol.* **2006**, *40*, 3775–3781.
4. Foote, C.S.; Wesler, S.; Corey, E.J.; Taylor, W.C. Olefin oxidation with singlet oxygen. *J. Am. Chem. Soc.* **1964**, *86*, 3879–3881.
5. Zepp, R.G.; Braun, A.M.; Hoigné, J.; Leenheer, J.A. Photoproduction of the hydrated electron from natural organic solutes in aquatic environments. *Environ. Sci. Technol.* **1987**, *21*, 485–490.
6. Larson, R.A.; Weber, E.J. Environmental Photochemistry, Chapter 6. In: *Reaction Mechanisms in Environmental Chemistry*; Lewis Publishers: Boca Raton, FL, USA, 1994.